Direct Numerical Simulation of the Bursting of a Laminar Separation Bubble and Evaluation of Flow-Control Strategies

Olaf MARXEN [1], **Dan S. HENNINGSON** [2]

[1] *Center for Turbulence Research, Stanford University, Stanford, CA 94305-3035, USA, email: olaf.marxen@stanford.edu*

[2] *Department of Mechanics, Royal Institute of Technology (KTH), SE-10044 Stockholm, Sweden*

Abstract. Direct numerical simulations of a short laminar separation bubble and its bursting are carried out. The bubble is developing on a flat plate due to an externally imposed pressure gradient. Laminar-turbulent transition in this bubble is triggered by small disturbance input with fixed frequency. The short bubble with disturbance input reaches a statistically steady state, while switching off this input yields a growing separation bubble. This phenomenon is denoted as bubble-bursting process. Disturbance input does not only prevent bursting, but can also serve to control the bubble size, which decreases with increased disturbance amplitude. Forcing at two different frequencies in the form of a beat is applied to control skin-friction and pressure distribution more independently.

Keywords: laminar-turbulent transition, instability, separation, DNS, flow control

1. Introduction

A laminar separation bubble (LSB) can originate if an initially laminar boundary layer is subject to a sufficiently strong adverse pressure gradient, and laminar-turbulent transition occurs in the detached shear-layer. Further downstream, the turbulent flow often reattaches in the mean, forming a closed bubble.

LSBs can be observed on laminar wing profiles or on high-lift devices to name but two examples. In environments with low disturbance levels, the transition process in a LSB is typically governed by a strong amplification of high-frequency, 2-d or weakly oblique fluctuating disturbances.

1.1. Bursting of Laminar Separation Bubbles

Owen and Klanfer [15] were the first to distinguish between short and long LSBs. Their classification is based on the bubble length in comparison to the chord of an airfoil. Tani [21] introduced a classification of long and short LSBs depending on whether their influence on the pressure distribution is local or global.

Under certain conditions, for slight changes in flow conditions, short bubbles can break-up into long ones, so-called bubble bursting. For bodies of finite dimension like airfoils, the flow might not reattach at all. This can lead to stall [13]. On a semi-infinite flat plate, the flow will finally reattach in any case. Laminar-turbulent transition plays a key role for reattachment of a short LSB. This suggests an interconnection of transition and bubble bursting. Even though laminar-turbulent transition in LSBs has been the subject of numerous studies in the past, both experimentally [9, 22] and numerically [1, 6, 12, 20], flow dynamics of bubble bursting is not yet well understood.

Gaster [5] carried out an investigation to settle characteristics of short and long bubbles and to develop a bursting criterion based on a pressure-gradient parameter and a local Reynolds number. Pauley et al. [16] suggested that bubble bursting coincides with the onset of vortex shedding in an otherwise fully steady separation bubble. Diwan et al. [3] introduced the height of the bubble as an additional parameter. However, none of the criteria have found general acceptance so far [3].

Recently, Marxen and Henningson [11] considered bursting as a dynamical process. They suggested to distinguish between two different forms of bubble bursting, depending on whether the long-bubble flow at reattachment is laminar as in [16] or turbulent as in [5]. Here, we concentrate on the latter case.

1.2. Flow Control of Laminar Separation Bubbles

Control of laminar separation using zero-net mass flux (ZNMF) devices on the surface of airfoils is a common approach. It has been applied to airfoils operating at low to medium Reynolds numbers and to flow over flat plates with imposed pressure gradient in laboratory-type investigations. Both, numerical [4, 8, 17, 18] and experimental [2, 19] models have been used. For unsteady blowing/suction using ZNMF devices, ongoing physical processes in such flows can be diverse, spanning from convective-type instability [17] to vortex-wall interaction [18].

2. Physical Model and Numerical Method

The basic configuration in this article is given by a flat-plate boundary layer at a sufficiently high Reynolds number subjected to a streamwise pressure gradient. Qualitatively, the set-up is similar to the one used in [5] or [9]. A pressure gradient is induced via the streamwise velocity at the upper boundary. The resulting pressure distribution changes downstream from strongly favourable to strongly adverse, which is not uncommon in applications. In a laboratory experiment, such a pressure gradient could be caused by putting a displacement body into the flow at some distance from the plate as e.g. in [9].

Table 1. Resolution used for DNS.

MMAX	NMAX	KMAX + 1	IMAX	LPER
769	3501	72	2	900

2.1. NUMERICAL METHOD

Direct numerical simulations (DNS) are carried out based on the three-dimensional unsteady Navier-Stokes equations in vorticity-velocity formulation for an incompressible fluid. The computational code was developed at the Institut für Aerodynamik und Gasdynamik (IAG), Universität Stuttgart. Further details, i.e. discretisation, numerical method, and implementation, can be found in [7, 14].

A Cartesian coordinate system with streamwise x, wall-normal y and spanwise dimension z is located at the wall. The method uses finite differences of fourth/sixth-order accuracy for downstream (NMAX) and wall-normal (MMAX) discretisation. Grid stretching (only) in wall-normal direction allows to cluster grid points m near the wall according to the following formula ($1 \leq \mathsf{m} \leq \mathsf{MMAX}$), with κ=0.15:

$$y_{\mathsf{m}} = y_{max}\left((1-\kappa)\cdot\left(\frac{\mathsf{m}-1}{\mathsf{MMAX}-1}\right)^3 + \kappa\cdot\left(\frac{\mathsf{m}-1}{\mathsf{MMAX}-1}\right)\right). \qquad (1)$$

In spanwise direction, a spectral Fourier ansatz is applied (KMAX + 1 modes) for complex modes (IMAX=2). An explicit fourth-order Runge-Kutta scheme is used for advancing a vorticity-transport equation in time with LPER time steps per fundamental period T_0. The solution of a Poisson equation for the wall-normal velocity is obtained by a direct method based on a Fourier expansion. A grid study [10] confirmed the resolution given in Table 1 to be sufficient.

2.2. NON-DIMENSIONALISATION AND BOUNDARY CONDITIONS

All quantities are non-dimensionalised using a reference length L_{ref}=$1.16 \cdot \delta^*_{ifl}$, derived from the displacement thickness δ^*_{ifl} at the inflow, and the free-stream velocity U_∞ at the inflow. The global Reynolds number Re=$U_\infty L_{ref}/\nu$ amounts to 600, corresponding roughly to the local Reynolds number based on the displacement thickness at x=0. At the inflow boundary x_{ifl}=-320 a Blasius similarity solution is prescribed with a Reynolds number based on the displacement thickness $Re_{\delta^*_{ifl}}$=515.02.

Upstream of the outflow boundary, which is located at x_{ofl}=441.905, a damping zone smoothly returns the flow to a steady laminar state. The useful region

of the integration domain extends up to $x \approx 380$. At y=0 a no-slip wall is placed. Flow through this wall does only occur within a disturbance strip (see below). Wall-normal height of the integration domain y_{max} is chosen to be 160. At the upper boundary, vorticity components are set to zero and the streamwise velocity u is set according to the following formula:

$$u(y_{max}) = 1 + a_1 \cdot exp(-b_1 x^2) + a_2 x^2 \cdot exp(-b_2 x^2), \tag{2}$$

with the choice a_1=10.0, a_2=-41.0, b_1=200.0, and b_2=12.0. In the homogeneous direction z the flow is assumed periodic with a spanwise extent λ_z=52.360.

Simulations are performed with deterministic disturbance input. A pair of oblique time-harmonic perturbations is triggered via blowing and suction at the wall through a ZNMF disturbance strip. The streamwise location of the strip is $x \in [x_s$=$1.5238, x_e$=$15.4558]$. Forcing is prescribed for each wave of the pair separately within the strip, with a velocity amplitude perpendicular to the surface distributed as

$$\hat{v}_{wall} = A_v/U_\infty(\tilde{x}^7 - 3\tilde{x}^5 + 3\tilde{x}^3 - \tilde{x})/0.238, \quad \tilde{x} = 2(x - \frac{x_e + x_s}{2})/(x_e - x_s). \tag{3}$$

Amplitude A_v and circular frequency β=$2\pi/T$=$2\pi f$ for the wall-normal velocity will be specified below for each case, respectively. Fundamental spanwise wavenumber for the disturbances is γ_0=0.12 in all cases. An initial condition is composed of a blending of a slip-flow (see section 3.1.) and a Blasius boundary-layer solution.

3. Direct Numerical Simulations of Bubble Bursting

A DNS of a short LSB shall serve as a reference for application of flow control. Results from this reference DNS will be described in section 3.2. However, to visualise the set-up we consider a two-dimensional slip flow for the same basic configuration first (section 3.1.).

3.1. SLIP FLOW

Replacing the lower boundary by a slip wall, the resulting slip-flow field u_{slip}, v_{slip} resembles a potential flow created by a cylinder (i.e. a dipole) above a wall [10]. A strong acceleration of the flow along the wall is followed by a strong deceleration. The streamfunction gives a good visualisation of the configuration (Fig. 1).

This slip flow does not only serve to generate an initial condition for DNS or to visualise the configuration. It will also be used for comparison with DNS with respect to the corresponding wall-pressure coefficient.

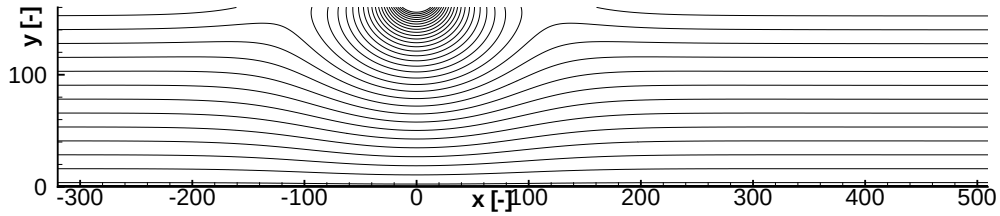

Figure 1. Contours of the stream function for slip flow.

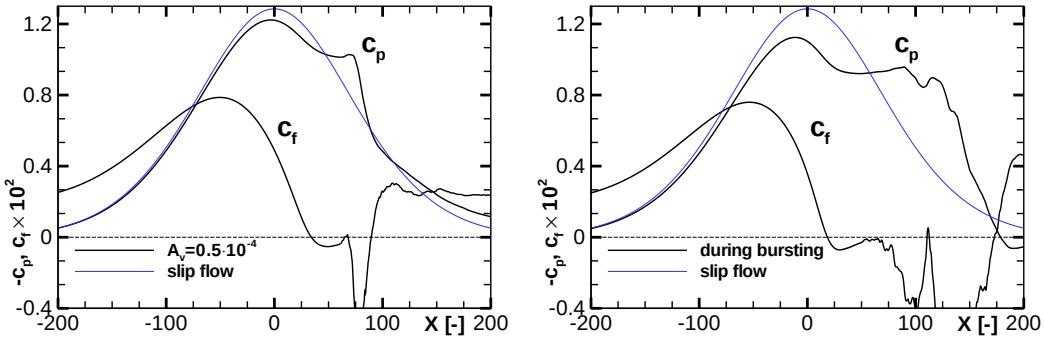

Figure 2. Coefficients for surface pressure c_p and skin-friction c_f. Left: Comparison of slip-flow results (thin, blue) and time-averaged DNS reference results with A_v=10^{-4} (thick). Right: Comparison of slip-flow results (thin, blue) and DNS results during bursting (thick) after disturbance input has been switched off around t=$46T_0$, time-averaged over the interval $[81T_0, 85T_0]$.

3.2. Reference Separation Bubble and its Bursting

A single pair of oblique waves is forced via the disturbance strip with an amplitude A_v=$0.5 \cdot 10^{-4}$. Fundamental frequency of this mono-harmonic forcing is β_0=0.3. It is among the most amplified frequencies according to linear stability theory and its amplification agrees well with the theory (see Fig. 5 in [11]). The computation is advanced until a statistically steady state has been reached. More details on this case can be found in [10, 11].

Wall-pressure coefficient c_p is seen to deviate from the case of slip flow only in the vicinity of the LSB (Fig. 2, left). This is in agreement with the expectation that a short LSB has only a local and limited effect on the potential flow. Furthermore, the formation of a pressure plateau is clearly seen in the region $50<x<80$. The skin-friction coefficient at the wall c_f (Fig. 2, left) reveals the separation location to lie at $x_S \approx 34$, while the flow reattaches in the mean at $x_S \approx 89$.

Gradually switching off disturbance input between t=$45T_0$ and t=$47T_0$ initi-

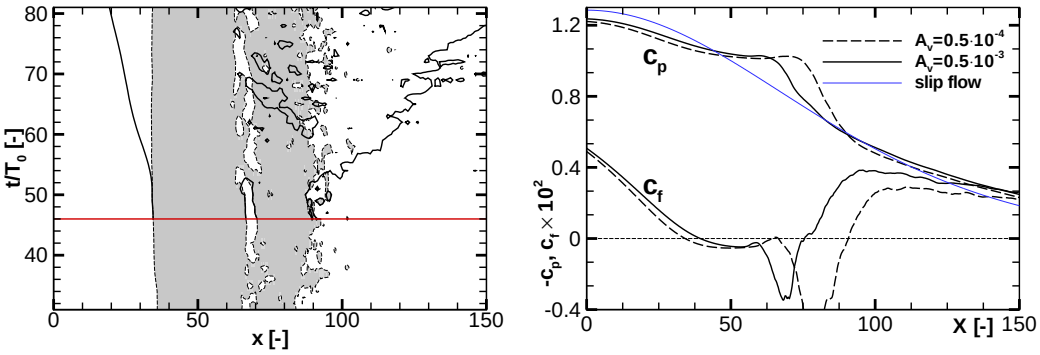

Figure 3. Left: Contours of vanishing skin-friction at the wall for a simulation where disturbance input was switched off around t/T_0=46 (solid line). Grey contour gives the region of negative skin friction in reference DNS with A_v=10^{-4}. Right: Coefficients for surface pressure c_p and skin-friction c_f. Comparison between DNS results with A_v=10^{-3} (solid) and reference DNS with A_v=10^{-4} (dashed).

ates a continuously growing separation bubble (Fig. 3, left). Eventually the reattachment point has moved considerably further downstream and influence on the pressure distribution is much stronger (Fig. 2, right). This process of deviation from the initially statistically-steady state shall be denoted as the bubble-bursting process. It has not yet stopped at the end of the bursting simulation t=$85T_0$.

Clearly, disturbance input is essential to maintain a short bubble in the present case. For that reason, the disturbance input can already be considered a means of flow control. On the other hand, its amplitude is so small that it can as well just be regarded as background noise instead.

4. Evaluation of Strategies for Separation Control

The last section has already demonstrated potential to control bubble bursting via unsteady ZNMF wall blowing/suction. As it was indicated there, the ZNMF actuator triggers an instability (of Kelvin-Helmholtz type) in the flow similar to the approach in [17]. However, below we will not only consider mono-harmonic forcing, but also forcing simultaneously at two different frequencies.

At first, we want to control the size of the corresponding short bubble (section 4.1.) by means of amplitude variation. However, if the control goal is to prevent bursting, triggering transition might not be required *continuously* due to a slow growth of the bubble from short to long state. Moreover, this might allow to control wall-pressure and skin-friction distribution more independently. Thus, one

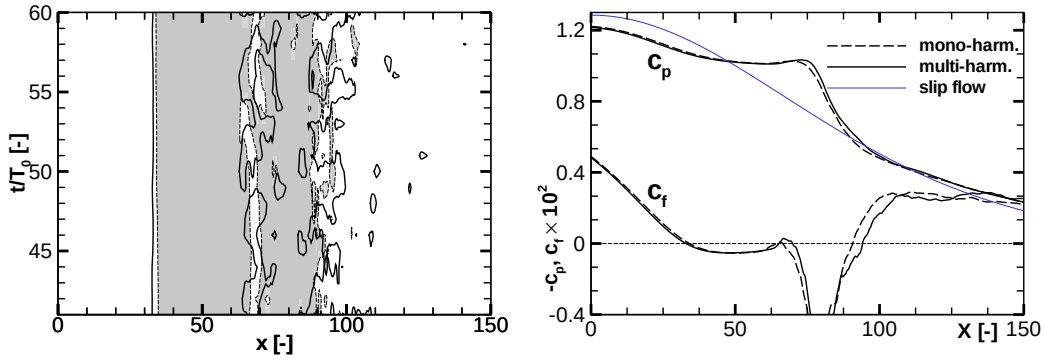

Figure 4. Left: Contours of vanishing skin-friction at the wall for multi-harmonic forcing (solid line). Grey contour gives the region of negative skin friction in reference DNS with A_v=10^{-4}. Right: Coefficients for surface pressure c_p and skin-friction c_f. Comparison between DNS with multi-harmonic forcing (solid) and reference DNS with A_v=10^{-4} (dashed).

could introduce a second, much lower frequency, e.g. in form of a beat (amplitude modulation) or a wave packet localised around the most unstable frequency in spectral space. The former approach will be considered here (section 4.2.).

4.1. CONTROLLABILITY OF BUBBLE SIZE

Ref. [17] applied unsteady, mono-harmonic ZNMF wall blowing/suction in a similar fashion as it is done here. In their conclusions, they posed the question whether their flow-control "method is sufficiently strong to prevent an "open separation"." If we increase disturbance amplitude by an order of magnitude compared to the reference DNS, we see the size of the (short) bubble decrease (Fig. 3, right). Therefore, the approach of [17] can be applied in our case where the bubble would undergo bursting, and thus become "open", if uncontrolled. Note that both, c_p and c_f, simultaneously react to flow control.

4.2. MULTI-HARMONIC FORCING

Growth of the separation bubble during bursting is a complex process in which the shear layer moves away from the wall while the reverse-flow region increases downstream and upstream. It can bee seen from Fig. 3 (left) that the time scale of this bursting process is much longer than the one of the instability. The latter is triggered in the simulations by forcing. This leads to the idea of a multi-harmonic forcing in the form of a beat. Such a forcing might be beneficial when the aim

is an overall reduction of pressure and skin-friction drag simultaneously. In this case it is desirable to control pressure and skin-friction distributions in a more independent way then it was done in section 4.1. Here, we just consider feasibility of this concept without looking in detail at the actual control gain.

Two pairs of oblique waves are forced via the disturbance strip with an amplitude A_v=$0.25 \cdot 10^{-4}$ each. Frequency of one of the wave pairs is β_1=0.27 while that of the other is β_2=0.33. This can be interpreted as forcing a single pair of oblique waves with β_0=0.3 similar to before but with a low-frequency amplitude modulation of frequency β_B=0.03=$1/10\beta_0$, and thus $A_v(t)$=$0.5 \cdot 10^{-4} \cdot cos(\beta_B t)$.

Differences between the reference case and multi-harmonic forcing are small. Both cases possess a very similar time evolution of skin friction (Fig. 4, left). Apparently, bursting is still prevented. Nevertheless, in the multi-harmonic case, patches of negative skin-friction are seen further downstream. These observations are confirmed if we look at time-averaged quantities. Both LSBs exhibit essentially the same pressure distribution, but in case of multi-harmonic forcing reattachment is shifted slightly further downstream (Fig. 4, right).

5. Conclusion

Time-dependent three-dimensional DNS of a flat-plate boundary layer subject to a strong favourable-to-adverse pressure gradient has been carried out. With small disturbance input, laminar-turbulent transition is triggered and a short laminar separation bubble develops. If disturbance forcing is switched off, the transition process is no longer able to immediately reattach the flow. As a result, a bursting process towards a long LSB sets in.

Increasing the forcing amplitude of such single-frequency forcing reduces bubble size. A feasibility study of forcing at two frequencies in the form of a beat indicates that pressure and skin-friction distribution are controllable in a slightly more independent way. Such multi-harmonic forcing might be favourable for separation-control strategies to prevent bursting with small energy input and to lower both pressure- and skin-friction drag.

Acknowledgements

O. Marxen gratefully acknowledges financial support by the Deutsche Forschungsgemeinschaft (German research foundation) under grant MA 3916/1-1 and computational time by the Höchstleistungsrechenzentrum (HLRS) Stuttgart, project *long_lsb*. Furthermore, he thanks Ulrich Rist and Markus Kloker, IAG, Universität Stuttgart for providing the DNS code *n3d*.

References

[1] M. Alam and N. D. Sandham. Direct Numerical Simulation of 'Short' Laminar Separation Bubbles with Turbulent Reattachment. *J. Fluid Mech.*, 410:1–28, 2000.

[2] J. P. Bons, R. Sondergaard, and R. B. Rivir. Turbine separation control using pulsed vortex generator jets. *J. Turbomachinery*, 123(2):198–206, 2001.

[3] S. S. Diwan, S. J. Chetan, and O. N. Ramesh. On the bursting criterion for laminar separation bubbles. In R. Govindarajan, editor, *Sixth IUTAM Symposium on Laminar-Turbulent Transition*, volume 78 of *Fluid Mechanics and Its Applications*, pages 401–407. Springer, Berlin, New York, 2006.

[4] H. F. Fasel and D. Postl. Interaction of separation and transition in boundary layers: direct numerical simulations. In R. Govindarajan, editor, *Sixth IUTAM Symposium on Laminar-Turbulent Transition*, volume 78 of *Fluid Mechanics and Its Applications*, pages 71–88. Springer, Berlin, New York, 2006.

[5] M. Gaster. The structure and behaviour of laminar separation bubbles. Number CP–4 in AGARD, pages 813–854, 1966.

[6] C. P. Häggmark, C. Hildings, and D. S. Henningson. A numerical and experimental study of a transitional separation bubble. *Aerosp. Sci. Technol.*, 5(5):317–328, 2001.

[7] M.J. Kloker. A Robust High-Resolution Split-Type Compact FD Scheme for Spatial Direct Numerical Simulation of Boundary-Layer Transition. *Appl. Sci. Res.*, 59:353–377, 1998.

[8] R.B. Kotapati, R. Mittal, O. Marxen, D. You, V. Kitsios, A. Ooi, and J. Soria. Harnessing resonant interactions for active control of separated flows. In *Proceedings of the 2006 Summer Program*, pages 445–456. Center for Turbulence Research, Stanford University, 2006.

[9] M. Lang, U. Rist, and S. Wagner. Investigations on controlled transition development in a laminar separation bubble by means of LDA and PIV. *Experiments in Fluids*, 36:43–52, 2004.

[10] O. Marxen and D. S. Henningson. Direct Numerical Simulation of a Short Laminar Separation Bubble and Early Stages of the Bursting Process. In *Contributions to the 15th STAB/DGLR Symposium, Nov. 29–Dec. 1, 2006, Darmstadt, Germany*. Accepted for publication, 2007.

[11] O. Marxen and D. S. Henningson. Numerical Simulation of the Bursting of a Laminar Separation Bubble. *AIAA Paper*, 2007-0538, 2007.

[12] O. Marxen, M. Lang, U. Rist, and S. Wagner. A Combined Experimental/Numerical Study of Unsteady Phenomena in a Laminar Separation Bubble. *Flow, Turbulence and Combustion*, 71:133–146, 2003.

[13] O. Marxen, D. You, and P. Moin. Numerical Simulations of the Bursting of a Laminar Separation Bubble and its Relation to Airfoil Stall. In *Proc. of the 11th EUROMECH European Turbulence Conference (ETC 11), June 25–28, 2007, Porto, Portugal*, 2007.

[14] D. Meyer, U. Rist, and M Kloker. Investigation of the flow randomization process in a transitional boundary layer. In E. Krause and W. Jäger, editors, *High Performance Computing in Science and Engineering '03*, pages 239–253. Transactions of the HLRS 2003, Springer, 2003.

[15] P. R. Owen and L. Klanfer. On the laminar boundary layer separation from the leading edge of a thin airfoil. Technical Report No. Aero 2508, Royal Aircraft Establishment, UK, 1953. In: A.R.C. Technical Report C.P. No. 220, 1955.

[16] L. L. Pauley, P. Moin, and W. C. Reynolds. The structure of two-dimensional separation. *J. Fluid Mech.*, 220:397–411, 1990.

[17] U. Rist and K. Augustin. Control of Laminar Separation Bubbles Using Instability Waves. *AIAA J.*, 44(10):2217–2223, 2006.

[18] M. P. Simens and J. Jimenez. Alternatives to Kelvin-Helmholtz instabilities to control separation bubbles. In *Power for Land Sea and Air*, ASME. Proceedings of ASME Turbo Expo 2006, Barcelona, Spain, May 8-11, 2006, 2006.

[19] R. Sondergaard, R. B. Rivir, and J. P. Bons. Control of low-pressure turbine separation using vortex-generator jets. *J. Propulsion and Power*, 18(4):889–895, 2002.

[20] P. R. Spalart and M. Kh. Strelets. Mechanisms of transition and heat transfer in a separation bubble. *J. Fluid Mech.*, 403:329–349, 2000.

[21] I. Tani. Low-speed flows involving bubble separations. *Prog. Aerosp. Sci.*, 5:70–103, 1964.

[22] J. H. Watmuff. Evolution of a wave packet into vortex loops in a laminar separation bubble. *J. Fluid Mech.*, 397:119–169, 1999.